Bioresource Technology 188 (2015) 145–152

Contents lists available at ScienceDirect

Bioresource Technology

journal homepage: www.elsevier.com/locate/biortech

Influence of mixotrophic growth on rhythmic oscillations in expression of metabolic pathways in diazotrophic cyanobacterium *Cyanothece* sp. ATCC 51142

S. Krishnakumar [a,1], Sandeep B. Gaudana [a,1], Madhuri G. Digmurti [a], Ganesh A. Viswanathan [a], Madhu Chetty [b], Pramod P. Wangikar [a,c,d,*]

[a] Department of Chemical Engineering, Indian Institute of Technology Bombay, Powai, Mumbai 400076, India
[b] School of Information Technology, Federation University Australia, Gippsland Campus, VIC 3841, Australia
[c] Wadhwani Research Center for Bioengineering, Indian Institute of Technology Bombay, Powai, Mumbai 400076, India
[d] DBT-Pan IIT Center for Bioenergy, Indian Institute of Technology Bombay, Powai, Mumbai 400076, India

HIGHLIGHTS

- Cultivation of *Cyanothece* 51142 under mixotrophy with ambient CO_2 and glycerol.
- Physiological, biochemical and gene expression analysis under mixotrophy.
- Respiratory/photosynthetic burst not observed in mixotrophy unlike photoautotrophy.
- Genes associated with N_2 fixation and H_2 production upregulated earlier.
- Insights for higher hydrogen production.

GRAPHICAL ABSTRACT

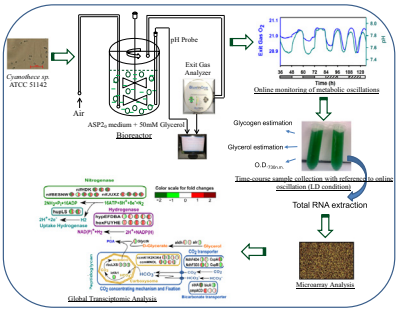

ARTICLE INFO

Article history:
Received 3 December 2014
Received in revised form 5 February 2015
Accepted 6 February 2015
Available online 16 February 2015

Keywords:
Transcriptomic analysis
Nitrogen fixation
Hydrogen production
Metabolic oscillations
Cyanobacteria

ABSTRACT

This study investigates the influence of mixotrophy on physiology and metabolism by analysis of global gene expression in unicellular diazotrophic cyanobacterium *Cyanothece* sp. ATCC 51142 (henceforth *Cyanothece* 51142). It was found that *Cyanothece* 51142 continues to oscillate between photosynthesis and respiration in continuous light under mixotrophy with cycle time of ~13 h. Mixotrophy is marked by an extended respiratory phase compared with photoautotrophy. It can be argued that glycerol provides supplementary energy for nitrogen fixation, which is derived primarily from the glycogen reserves during photoautotrophy. The genes of NDH complex, cytochrome c oxidase and ATP synthase are significantly overexpressed in mixotrophy during the day compared to autotrophy with synchronous expression of the bidirectional hydrogenase genes possibly to maintain redox balance. However, nitrogenase complex remains exclusive to nighttime metabolism concomitantly with uptake hydrogenase. This study throws light on interrelations between metabolic pathways with implications in design of hydrogen producer strains.

* Corresponding author at: Department of Chemical Engineering, Indian Institute of Technology Bombay, Powai, Mumbai 400076, India. Tel.: +91 2225767232.
E-mail address: wangikar@iitb.ac.in (P.P. Wangikar).
[1] These authors contributed equally.

http://dx.doi.org/10.1016/j.biortech.2015.02.016
0960-8524/

1. Introduction

Concerns regarding global warming and CO_2 emission have led to renewed interest in biological capture of CO_2. Cyanobacteria, a phylum comprising of oxygenic photosynthetic prokaryotes, are known for their significant role in nature's carbon and nitrogen cycles (Sherman et al., 2010). This group of photosynthetic organisms efficiently fixes atmospheric CO_2. Some cyanobacteria fix molecular nitrogen producing hydrogen (H_2) as a byproduct (Ghirardi et al., 2007; Prince and Kheshgi, 2005). Nitrogen fixation in cyanobacteria is deemed to be sensitive to oxygen (O_2) as nitrogenase gets irreversibly inactivated in presence of O_2. Therefore, unicellular and multicellular diazotrophic cyanobacteria strategically use temporal and spatial separation, respectively, to sustain oxygenic photosynthesis and oxygen-sensitive nitrogen fixation within the same organism (Reddy et al., 1993; Dean et al., 1993).

Cyanothece sp. ATCC 51142 (hereafter, *Cyanothece* 51142), is a unicellular nitrogen fixing cyanobacterium. This organism performs nitrogen fixation during dark to temporally separate it from oxygenic photosynthesis (Colon-Lopez et al., 1997). *Cyanothece* 51142 shows versatility in its ability to grow with or without nitrate, light and organic carbon source leading to growth under autotrophic, mixotrophic and heterotrophic growth conditions. Endowed with such extraordinary metabolic capabilities, *Cyanothece* 51142 has been considered as a promising organism for production of hydrogen (H_2) (Bandyopadhyay et al., 2013).

Cyanothece 51142 stores the fixed carbon as glycogen granules during daytime, which are then used as a substrate during the nighttime nitrogen fixation by providing necessary ATP molecules at the expense of accumulated glycogen granules (Schneegurt et al., 1994). Transcriptomic analysis of the culture under photoautotrophic growth uncovered orchestration of genome-wide diurnal oscillations in metabolic pathways (Stockel et al., 2008; Toepel et al., 2008; Elvitigala et al., 2009). Subsequently, sustained oscillations in gene expression were demonstrated under constant light (Cerveny et al., 2013; Gaudana et al., 2013; Krishnakumar et al., Unpublished results). *Cyanothece* 51142 is noted for its remarkable ability to produce hydrogen under mixotrophic conditions with glycerol as substrate and under nitrogen fixing conditions (Min and Sherman, 2010). High cell density cultivation of *Cyanothece* 51142 to 8.4 g L^{-1} final biomass under mixotrophic condition was recently reported (Alagesan et al., 2013). However, there has not been much focus on genome-wide transcriptomic and proteomic studies on this organism under mixotrophy, which can be instrumental in devising strategies for strain improvement.

In the present work, physiological, biochemical and global transcription changes in *Cyanothece* 51142 are analyzed, for the combined effect of glycerol and ambient atmospheric CO_2, under diurnal cycles. Interestingly, significant changes are observed in the global gene expression profiles when the growth medium is supplemented with glycerol. In addition to transcriptional analysis, online measurements such as medium pH, exhaust gas CO_2 and O_2, and biochemical analysis were performed under LD as well as constant light (LL) to substantiate the physiological and metabolic activity of the organism as well as to gain insights for ensuing bioprocess engineering in strains belonging to genus *Cyanothece*.

2. Methods

2.1. Bacterial strain and culture conditions

Axenic culture of *Cyanothece* sp. ATCC 51142 was grown and maintained in ASP2 medium with 1.5 g l^{-1} $NaNO_3$ at 30 °C as described previously (Reddy et al., 1993). The culture was maintained under an illumination intensity of 50 μEinstein m^{-2} s^{-1} in an orbital shaker-incubator (Orbitek, Chennai, India) at 120 rpm (rpm) and 30 °C.

2.2. Photo-bioreactor setup and growth conditions

Cells grown to mid-log phase were washed with 0.85% NaCl and re-suspended in $ASP2_0$ (ASP2 medium without nitrate) and inoculated in 1.5 L $ASP2_0$ supplemented with 50 mM glycerol in 2 L Biostat B plus bioreactor maintained at 30 °C (Sartorius, Gettingen, Germany). The culture was illuminated externally using 40 W cool white fluorescent lamps (Oreva, Ahmedabad, India) to provide a surface light intensity of 300 μM m^{-2} s^{-1} inside the bioreactor. The agitation was maintained at 600 rpm using 6-blade disk impellers. For aeration, 0.2 micron filtered atmospheric air was continuously sparged from the bottom of the reactor at a flow rate of 0.1 volume of air/volume of medium/min (vvm) (Krishnakumar et al., 2013). The exit gas was analyzed for volume percentage of CO_2 and O_2 using BlueInOne Cell exit gas analyzer (BlueSens, Herten, Germany) with data being recorded at every one minute interval and the pH of the growth medium was measured using a pH probe (Hamilton, Bonaduz, Switzerland). The culture was entrained with three diurnal cycles with each cycle of 12 h light and 12 h dark phases (LD) and then released in constant light (LL).

2.3. Harvesting of culture and sample analysis

Samples were drawn aseptically to measure optical density of the culture at 730 nm (OD_{730}), intracellular glycogen content and to extract total RNA, at the following time points from the time of inoculation: 49 h, 53 h (1 h and 5 h into the light phase, respectively), 61 and 65 h (1 h and 5 h into the dark phase, respectively). Since the culture grows faster under mixotrophy than under photoautotrophy, the initial inoculum was kept about 3-fold lower under mixotrophy and the entrainment period under LD was cut down from 4 days that was used for photoautotrophy (Gaudana et al., 2013) to 3 days in the current study. Intracellular glycogen content was estimated as described earlier (Krishnakumar et al., 2013). Briefly, 1 ml methanol was added to cell pellet, incubated for 15 min in a water bath preset at 60 °C, cooled down to room temperature and centrifuged at 12,000*g* for 10 min. Thereafter free glucose was removed by adding 100 μl 40% KOH to the pellet and incubating at 95 °C for 1 h. Glycogen was precipitated by addition of 200 μl of absolute ethanol and overnight incubation at −20 °C followed by centrifugation at 12,000*g* for 1 h at 4 °C. Glycogen was chemically hydrolyzed by addition of 2 N HCl and incubation at 95 °C for 30 min. Solution was neutralized by addition of 40 ml of 2 N NaOH, 20 ml of 1.0 M phosphate buffer (pH 7.0), and 40 ml of distilled water and vortexing thoroughly. Released glucose was estimated Glucose GOD PAP kit, a Glucose oxidase based enzyme assay kit (Biolab Diagnostics (I) Pvt. Ltd., Boisar, India) as per the manufacturer's instructions. Glycogen content in the samples was calculated based on standard plot using known quantities of commercially procured glycogen.

2.4. RNA extraction, real time PCR and microarray analysis

Total RNA was extracted from the cells using TRIzol reagent (Life Technologies, Grand Island, USA) as described previously (Gaudana et al., 2013). Briefly, cells were frozen at −80 °C with 1 ml of TRIzol reagent immediately after collecting the sample, till the time of extraction. Cells were thawed on ice just before initiating total RNA extraction. Cells were lysed using 500 μm acid washed glass beads and 4 rounds of vortexing with intermittent incubations on ice for 30 s each. RNA samples from 47 h, 49 h, 59 h and 61 h were used for microarray analysis. Additionally,

two samples, 1 h each into the light and the dark phases, were drawn from cells growing under photoautotrophy, but otherwise the same growth conditions. The control comprised of pool of equimolar RNA of 4 samples from mixotrophy and 2 samples from photoautotrophy as described above. Microarray analysis was carried out at MoGene (St. Louis, USA) as described earlier (Stockel et al., 2008; Krishnakumar et al., Unpublished results). Briefly, total RNA from individual samples and an equi-molar mixture of all samples as control were labeled with Cy3 and Cy5, respectively. Unbound dyes were removed using RNA clean kit (Zymo Research, Irvine, CA). Labeled RNA samples were hybridized on Agilent-018970 Cyanothece 51142 custom 8 × 15 K array slides spotted with single 60-mer oligonucleotide probes for each of the 5304 ORFs of *Cyanothece* 51142 Two biological replicates, two technical replicates and a dye swap were analyzed for each sample from individual time points. The results are from 2 independent biological replicates and 2 technical replicates. Real time PCR (RT-PCR) analysis was carried out for a select number of genes for validating the microarray data (Table 1), using gene specific primers as described earlier (Gaudana et al., 2013) with minor modifications. Briefly, 1 μg of total RNA sample from each time point was reverse transcribed using Enhanced Avian RT First strand synthesis kit and random oligomers (Sigma–Aldrich, St Louis, USA). Quantitative RT-PCR was carried out using LuminoCT SYBR green qRTPCR mix (Sigma–Aldrich) on Eco Real-time PCR system (Illumina, San Diego, USA).

2.5. Glycerol estimation

Concentration of glycerol was estimated by HPLC analysis using HP-Aminex-87-H column (Bio-Rad, Hercules, USA) and RI detector L-7490 (Merck-Hitachi, Darmstadt, Germany). Sample was collected by centrifuging 1 mL of culture at various time points, as mentioned in Section 2.1 and then transferring the supernatant to a fresh vial. To analyze the sample, the temperature of the column was maintained at 65 °C and a mobile phase with concentration of 5 mM sulfuric acid was constantly passed at a flow rate of 0.6 mL per minute.

2.6. Visualization of transcriptomic data

SVG mapping tool (Leplat et al., 2013) was used to visualize the transcriptomic data of the present study. For this, a pictorial layout with all metabolic pathway information was drawn using inkscape vector graphics tool and then mapped to the transcriptomic data. For labeling the genes in the pictorial layout, the standard KEGG pathway database was used as a reference.

3. Results and discussion

3.1. Dynamics of growth parameters

Under mixotrophic growth, online profiles of pH and exhaust gas CO_2 and O_2 showed rhythmic oscillations under both LD and LL (Fig. 1). For oscillations under LL, the culture showed significant differences in amplitude and periodicity compared to that reported for photoautotrophic growth (Cerveny and Nedbal, 2009; Krishnakumar et al., 2013; Gaudana et al., 2013). Firstly, the culture shows a cycle time of ~13 h under mixotrophy compared to that of ~11 h under photoautotrophy. Secondly, amplitude of the CO_2 burst increased for each subsequent cycle possibly due to an increase in cell density. Further, the metabolism sees oscillations between two phases; low net respiration (low exhaust gas CO_2 levels) and high net respiration (high CO_2 levels) and the culture does not engage in net CO_2 capture even during the low CO_2 phase. It can be argued that the culture engages in photosynthesis during the low net respiration phase and not during the high respiration phase. In contrast, there is net CO_2 capture for about half of the 11 h cycle under autotrophy under LL. Moreover, the respiratory bursts last longer under mixotrophy both under LD and LL compared to the corresponding phases under photoautotrophy. The longer periods of respiration seem to be powered by glycerol, an organic carbon source that is readily taken up by the organism (Feng et al., 2010).

In synchrony with the online exit gas profiles, the glycogen content increased during the light phase and declined sharply during the dark phase till the 3rd day of LD. These oscillations cease subsequently possibly as the presence of glycerol alleviates the need for internal storage of energy molecules. This is strikingly different from what was observed under photoautotrophic growth where there is a complete synchrony between the rhythmicity in profiles of exit gas, pH of the medium, cell growth and glycogen content. Further, the increased cell density during mixotrophy may lead to self-shading thereby resulting in an increased fraction of energy derived from glycerol during subsequent cycles of oscillation under LL conditions.

3.2. Insights from transcriptomic analysis

A detailed genome scale transcriptomic analysis was performed to understand the systematic metabolic changes in *Cyanothece* 51142 under nitrogen fixing mixotrophic growth condition under a diurnal cycle. Heatmap of the gene expression data from the present study along with that reported for photoautotrophy (Stockel et al., 2008) shows that majority of the day peaking genes show similar behavior under the two growth modes. However, a significant fraction of the genes including those involved in nitrogen fixation, hydrogen production, cytochrome C complex synthesis and assembly, cobalamin biosynthesis, ferrous and molybdenum transport, that peak at night during photoautotrophy peak at mid-day under mixotrophy (Fig. 2). Detailed analysis of the comparison and contrasts in gene expression under these two growth conditions and their implications are discussed in the following sections.

Signatures of gene expression pattern for many vital cellular activities were analyzed, through mapping the transcriptomic data with the respective genes using SVG mapping. Transcriptomic data for photoautotrophic condition from (Stockel et al., 2008) was mapped similarly to bring out the key metabolic differences between these two growth modes.

3.2.1. Nitrogen fixation and hydrogen production

Analysis of the transcript abundance of nitrogenase and hydrogenase related genes in *Cyanothece* 51142 revealed interesting metabolic changes in the cellular system under mixotrophic growth. For instance, the nitrogenase complex genes, that is the structural *nifHDK* genes and the associated nine accessory genes (*nifB*, *nifE*, *nifS*, *nifN*, *nifW*, *nifJ*, *nifU*, *nifX*, *nifZ*) showed synchronized expression starting with an upregulation around mid-day as opposed to dusk peaking under photoautotrophy (Fig. 3). Particularly, *nifJ*, which is a gene coding for pyruvate oxidoreductase (Schmitz et al., 1993), showed strong upregulation early in the day in contrast to that under photoautotrophic growth, wherein it is up-regulated only in dark (Fig. 3). This probably could be due to functional role of this gene in generating reducing equivalents required for the N_2 fixation. The genes coding for cyanophycin (multi-L-arginyl-poly-L-aspartic acid) granules, which serve as nitrogen storage molecules and known to peak in the dark under photoautotrophy, interestingly showed a metabolic shift with concerted up-regulation around mid-day (Fig. 3). In synchrony with the gene expression, the online profiles such as pH, and exit gas

Table 1
Validation of microarray data employing qRT-PCR.

		Fold change from microarray data*				Fold change from qRT-PCR data*			
		Time (h)				Time (h)			
Locus tag	Gene	49 h	53 h	61 h	65 h	49 h	53 h	61 h	65 h
cce_4751	cikA	**1.55**	0.71	1.27	1.29	**1.96**	0.01	0.59	0.02
cce_0424	kaiA	**1.69**	1.68	0.99	1.45	**1.87**	0.01	0.59	0.02
cce_0423	kaiB1	**1.92**	1.05	0.6	1.64	**1.29**	0.05	0.37	0.18
cce_0422	kaiC1	0.82	**0.87**	0.3	0.69	0.05	**1.26**	0.12	0.14
cce_4716	kaiC2	0.89	**1.16**	1.26	0.57	0.05	**0.89**	0.49	0.08
cce_1751	sasA	1.08	1.03	**1.78**	0.91	0.19	0.01	**43.79**	0.01
cce_3166	rbcL	**1.72**	1	0.27	1.05	**1.38**	0.21	0.20	1.21
cce_3974	glpX	**1.7**	1.52	0.36	0.78	**1.64**	0.04	0.13	0.21
cce_4283	ccmK2	**1.72**	1.01	0.27	0.84	**1.45**	0.25	0.4	1.02
cce_0559	*nif*H	0.26	0.01	**3.3**	1.59	0.02	0.04	**32.43**	0.02

* Fold change at the time point when a particular gene peaks is emphasized using bold font. The peak times for most genes match for microarray and qRT-PCR datasets, validating the former as described earlier (Stockel et al., 2008).

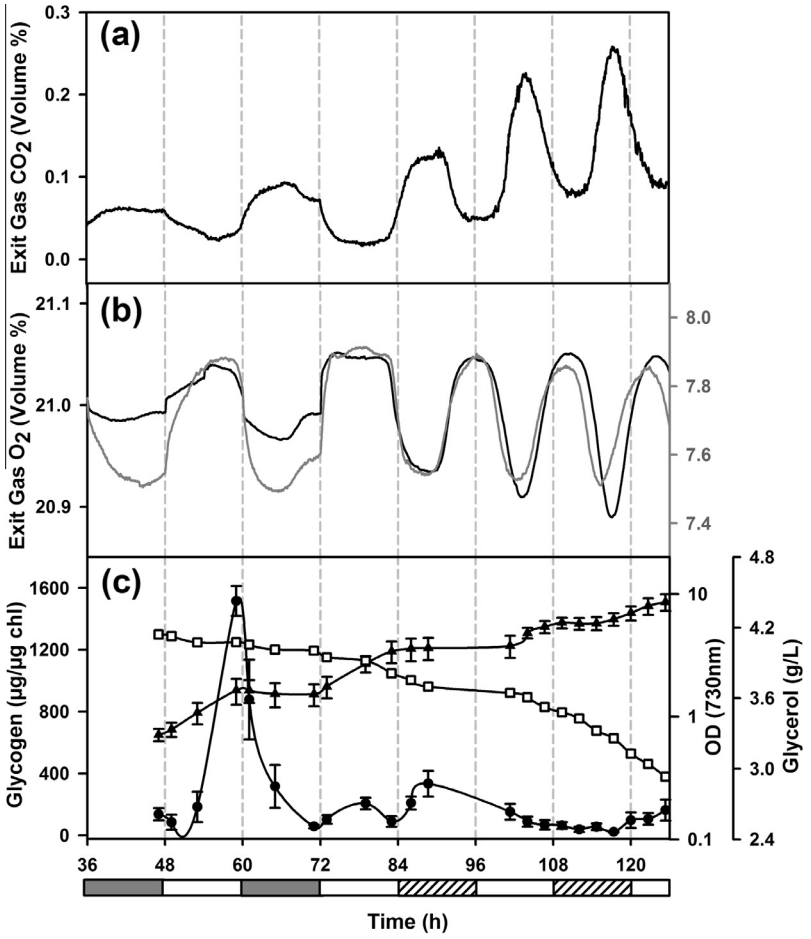

Fig. 1. Metabolic oscillations of *Cyanothece* 51142 under mixotrophic growth condition. *Cyanothece* 51142 was grown in nitrate-limited supplemented with 50 mM glycerol first under diurnal cycles (LD) for three days and then released in continuous light (LL). (a) exhaust gas CO_2 profile, (b) exhaust gas O_2 profile (black) and pH of the medium (gray) and (c) profiles of intracellular glycogen (●), glycerol (▲) and optical density (OD at 730 nm) to indicate culture density (□). Shading of the rectangular boxes below the *X*-axis indicate light (white box), dark (dark gray box) and subjective dark in continuous light (shaded). The online profile is shown for a representative experimental run from 4 biological replicates resulting in similar online profiles.

O_2 dipped and exit gas CO_2 peaked earlier before the onset of dark (Fig. 1a and b) as compared to that under photoautotrophy (Gaudana et al., 2013).

Similarly, the uptake hydrogenase genes: *hupL* and *hupS* as well as the genes coding for hydrogenase: *hypA*, *hypB*, *hypF*, *hypF* are upregulated around mid-day under mixotrophy. The hydrogen (H_2) production is a means of replenishing the reducing equivalents (e^-), lost during N_2 fixation, photosynthesis maintenance and other reductive processes (Tamagnini et al., 2007). In case of photoautotrophy (Stockel et al., 2008), the hydrogenase genes exhibited up-regulation only in the dark regime. Probably, the presence of glycerol as an external carbon source might have effected this metabolic shift. In particular, the influence of glycerol and high light condition would have caused the over-production of

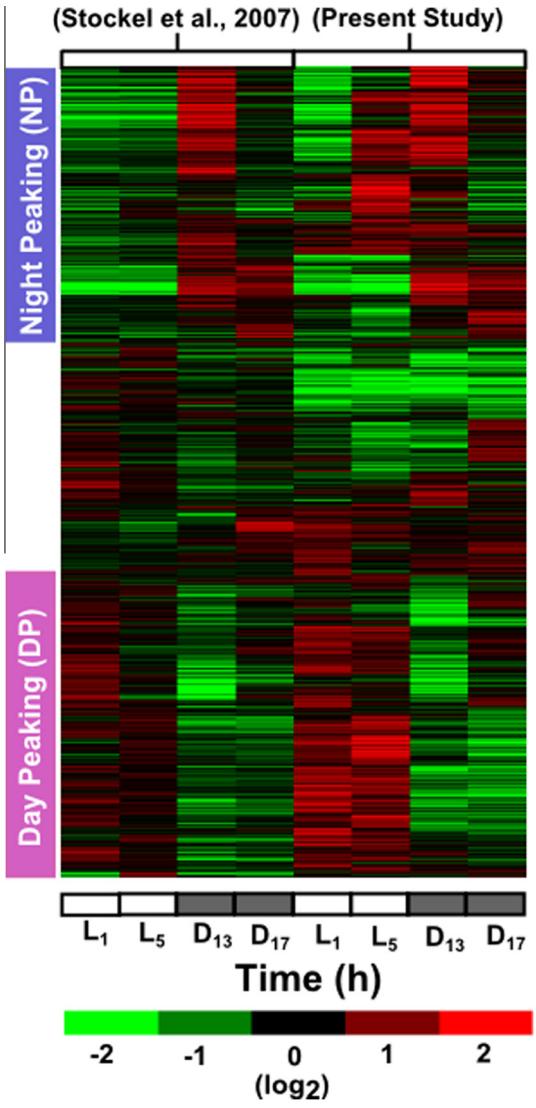

Fig. 2. Clustering analysis from microarray gene expression data of *Cyanothece* 51142 under nitrogen fixing conditions in photoautotrophy (data from Stockel et al., 2008) and mixotrophy (present study). Heat map was generated by performing hierarchial clustering for 1813 genes that satisfying 1.5-fold threshold, from the transcriptomic data of both Stockel et al., 2008 and the present study. An equivalent four time points, that is 1 h and 5 h into both light and dark phases, from both the transcriptomic data sets were considered for the analysis. Rectangular boxes in pink and blue on the *Y*-axis of the figure, represents the group of genes that peak during day and night, respectively. Color scale bar on the *X*-axis represents the range of log2 fold change gene expression values, where in red and green denotes the up-regulation and down-regulation of genes, respectively. (For interpretation of the references to color in this figure legend, the reader is referred to the web version of this article.)

NAD(P)H reductants. As a reason, Hox hydrogenase genes show strong expression in the day during carbon fixation and photosynthesis, especially to regulate the redox imbalance as suggested earlier (Carrieri et al., 2011; Tamagnini et al., 2007).

3.2.2. CO_2 fixation and glycerol metabolism

The genes involved in CO_2 fixation, such as *rbcL*, *rbcX* and *rbcS*, showed better expressions in photoautotrophy (Stockel et al. 2008) as compared to that in mixotrophy (Fig. 3). It is understood that the affluence of glycerol strongly limited the CO_2 uptake as compared to that under autotrophic growth where atmospheric CO_2 serves as the sole carbon source. Conversely, some representative genes such as *aldh*, and *glyctk* that are related to glycerol metabolism were observed to be up-regulated in the day time. This denoted that the organism proficiently takes part in glycerol consumption for its enriched growth and metabolism. Moreover, the glycerol metabolism genes were noticed as mostly either $NADP^+$ or NAD^+ dependent. In particular, these genes code for enzymes that transform glycerol into D-glycerate and then to glycerol-3 phosphate (G3P) with the assistance of ATP molecules (Fig. 4). Besides, the glycerol metabolism suggested that either it provides ATP molecules independently (Bandyopadhyay et al., 2010) or through glycogen that accumulated via CO_2 fixation and glycerol utilization.

3.2.3. CO_2 concentrating mechanism (CCM)

The expression of carbon concentrating mechanism (CCM) components in cyanobacteria is highly responsive to various growth parameters, particularly the availability of light and carbon source (Burnap et al., 2013). Interestingly, significant changes were observed in mixotrophic condition when compared to the gene expression under photoautotrophic growth for CCM components. For example, the operonic genes *ccmKLNO* encoding the shell proteins of carboxysomes (Kinney et al., 2011) have showed prolonged expression during the day.

Furthermore, the low affinity Ndh-1_4 (Price, 2011) complex seems to dominate in CO_2 uptake, as *cupA* gene showed induced transcription level upon illumination as compared to *cupB*. The genes coding for bicarbonate (HCO_3^-) transporters, that is, high affinity *cmpABCD* operon encoding bicarbonate translocase (BCT), high affinity Na^+-dependent SbtA and low affinity Na^+-dependent BicA were noticed to show insignificant changes in the cellular mixotrophic state. Of these, the *bicA* was completely downregulated and *sbtA* showed increased expression after 1 h into the light phase. For BCT transporter, only *cmpA* gene was upregulated during the day, which is reported to occur under Ci limitation or high light stress condition (McGinn et al., 2005).

3.2.4. Cell division

On analyzing cell division (*ftsZ*, *ftsY*, *ftsW*) and cell regulation (*ftsH1*, *ftsH2*, *ftsH3*, *ftsH4*) related genes, a higher and comparatively early expression was noted in mixotrophic growth than that under photoautotrophic growth. In particular, all the four copies of *ftsH* genes (*ftsH1H2H3H4*) highly up-regulated (Fig. 3), representing that cells actively engage in replenishing the impaired proteins and controlling of the protein degradation activities (Gottesman, 2003). Further, the essential cell division gene (*ftsZ*) peaked earlier upon illumination, which apparently indicated that it would lead to Z-ring formation followed by septum formation using other *fts* genes such as *ftsW*, *ftsA* and *ftsN* (Addinall and Lutkenhaus, 1996). In addition, the necessary GTPase activity of *ftZ* gene for inducing Z-ring formation was identified largely active in purine metabolism at early in the day time (Fig. 4). The up regulation of the genes involved in cell division also correlates with significantly high rate of growth as compared to that in otherwise same sets of growth conditions under photoautotrophy (Gaudana et al., 2013).

3.2.5. Effect of glycerol on electron transport chain (ETC)

To understand the glycerol effect on electron transport chain (ETC), representative genes that related to photosystem I, photosystem II, ATP synthase and redox carriers such as NDH complex, succinate dehydrogenase, plastoquinone (PC), cytochrome b6/f complex, plastocyanin and aa3-type cytochrome C oxidase were analyzed. Under mixotrophic condition, the electron donor NDH complex that located first in the ETC reported elevated transcript levels, while it shows lower gene expression in case of photoautotrophy (Stockel et al. 2008) (Fig. 3). The key reason for higher expression would be because of the availability of more reduced NAD(P)H molecules, due to increase in the carbon flux in the form

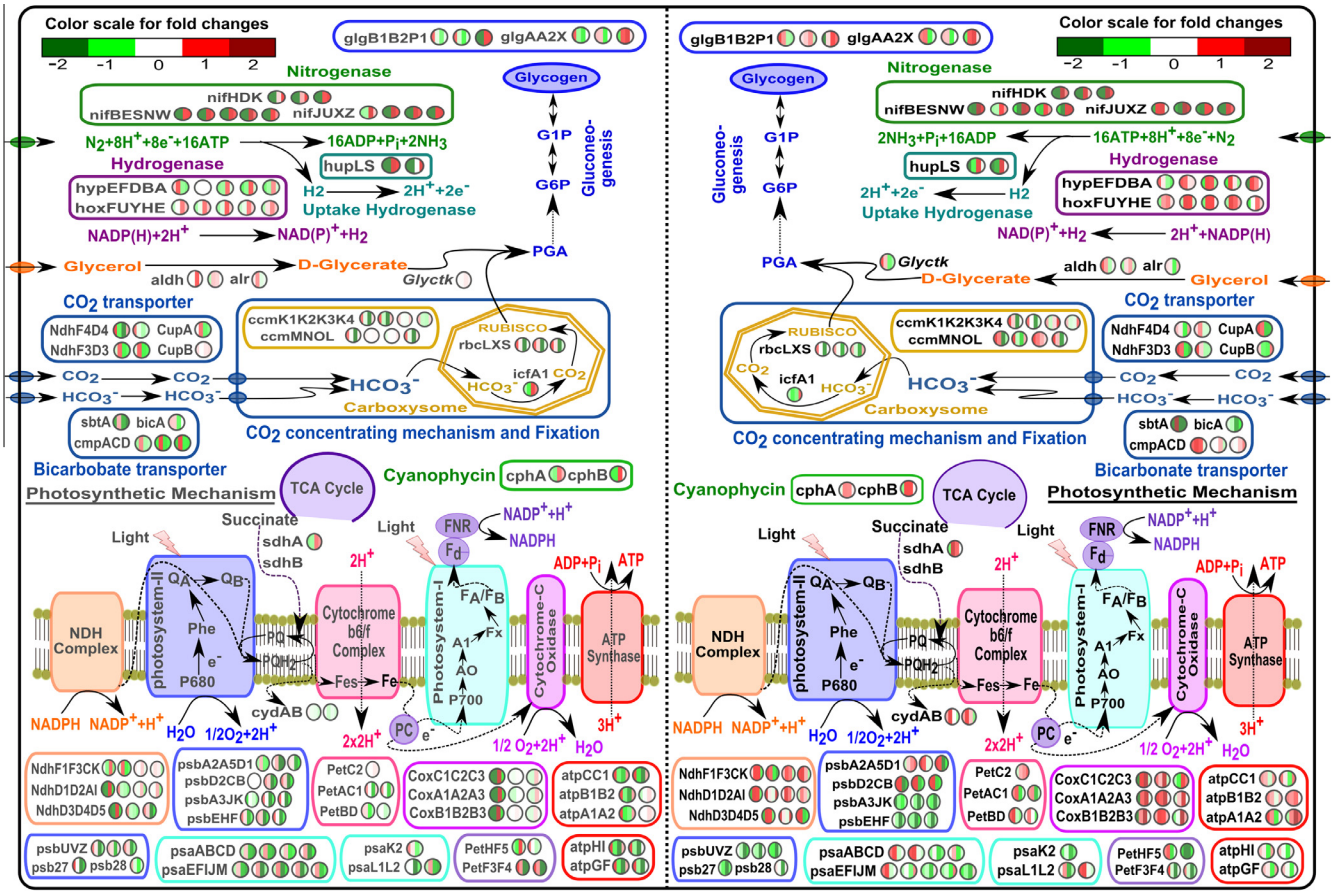

Fig. 3. Comparison of gene expression profiles of *Cyanothece* 51142 under nitrogen fixing conditions between photoautotrophy (left half of the panel; data from Stockel et al., 2008) and mixotrophy (right half of the panel; present study) for select metabolic pathways of carbon and nitrogen fixation, photosystems I and II and electron transport chain, constructed using SVG mapping tool. The filled circles in the pictorial layoutare color coded and divided in four parts to depict the expression of a gene at four time points; the left half of the circle represent 1 h and 5 h into light and the right half of the circle those in dark (i.e., 1 h, 5 h, 13 h and 17 h in an L/D diurnal cycle collected on the third day). The text that is linearly tagged to the circles denotes the standard acronyms for each of the individual genes. Operonic genes such as *nifH*, *nifD* and *nifK* are grouped together and denoted as *nifHDK* for brevity with the three circles representing expression of the genes in that order. Scale bar on the top represents the color code for fold change values. To exemplify, majority of the genes from *nif* gene cluster are downregulated during the day and upregulated at night. In the present study, the fold change is with respect to a pooled RNA sample of the four time points in mixotrophy and 1 h and 13 h samples in autotrophy. (For interpretation of the references to color in this figure legend, the reader is referred to the web version of this article.)

of glycerol to the cellular metabolism. Central metabolic pathways such as glycolysis and TCA cycle, a major resource of reduced NAD(P)H suppliers generally involves in contributing these molecules to NDH complexes for transferring electrons to photosystem II.

During photosynthesis, the light-induced photosystem PS-II demonstrated higher activity for structural photosystem genes (*psbD1*, *psbD2*, *psbC*, *psbB*, *psbA2* and *psbA5*), while the remaining secondary photosystem genes were altogether down-regulated (Fig. 3). Similar to the above, photosystem PS-I exhibited induced expression only for the core genes (*psaA*, *psaB*), and the rest PS-I genes except *psaL1* and *psaL2* showed down-regulation in the expression. In contrast, the photosystem genes for photoautotrophy (Stockel et al. 2008) showed moderate expression for most of the genes (Fig. 3). This evidently indicated that supplementation of glycerol significantly suppresses the secondary level genes of photosystem PS-II and PS-I, possibly due to self-shading resulting from higher cell density or lower atmospheric CO_2 fixation owing to glycerol as an additional carbon source or a combination thereof.

Plastoquinone (PQ) accepts electrons from both the ends of PS-II and succinate dehydrogenase and transfers the electrons to cytochrome b6f complex (Vermaas, 2001). It is also known that the cytosolic succinate dehydrogenase *sdhA* and *sdhB* contributes additional electrons to the plastoquinone by functioning as an electron donor (Cooley and Vermaas, 2001). Supportive of this, *sdhA* gene showed up-regulation prior to the dark, which highlighted the active involvement of succinate dehydrogenase in contributing extra electrons to PQ pool. In addition to plastoquinone, another set of electron carrier genes *cydA* and *cydB* encoding cytochrome bd quinol oxidase was observed to be upregulated, serving as an alternative route for transferring the electrons. In agreement to this, an induced expression of these genes was observed in the day, which stated that PQ might have involved in re-distributing the electrons to cytochrome bd quinol oxidase to circumvent the over-reduction of PQ pool (Pils and Schmetterer, 2001).

Notably, the electron carriers such as cytochrome b6/f complex and plastocyanin (PC) showed prolonged expression for structural core genes (*petB*, *petA*, *petC1*, *petC2* and *petH*). This denoted that these core genes play a crucial role in shuttling of the electrons to photosystem PS-I. Alternatively, the aa3-type cytochrome C terminal oxidase exhibited tightly-regulated expression in continuous fashion, where the expression started earlier in the mid-light phase for most of the Cox genes (*coxC2*, *coxA1*, *coxA2*, *coxA3*, *coxB1*and *coxB2*). This unquestionably stated that the organism involved in intense respiration under the presence of additional carbon source as suggested previously (Schmetterer et al., 2001). In contrast, the terminal oxidase Cox genes in photoautotrophy (Stockel et al. 2008) showed reduced expression and that too only in the dark.

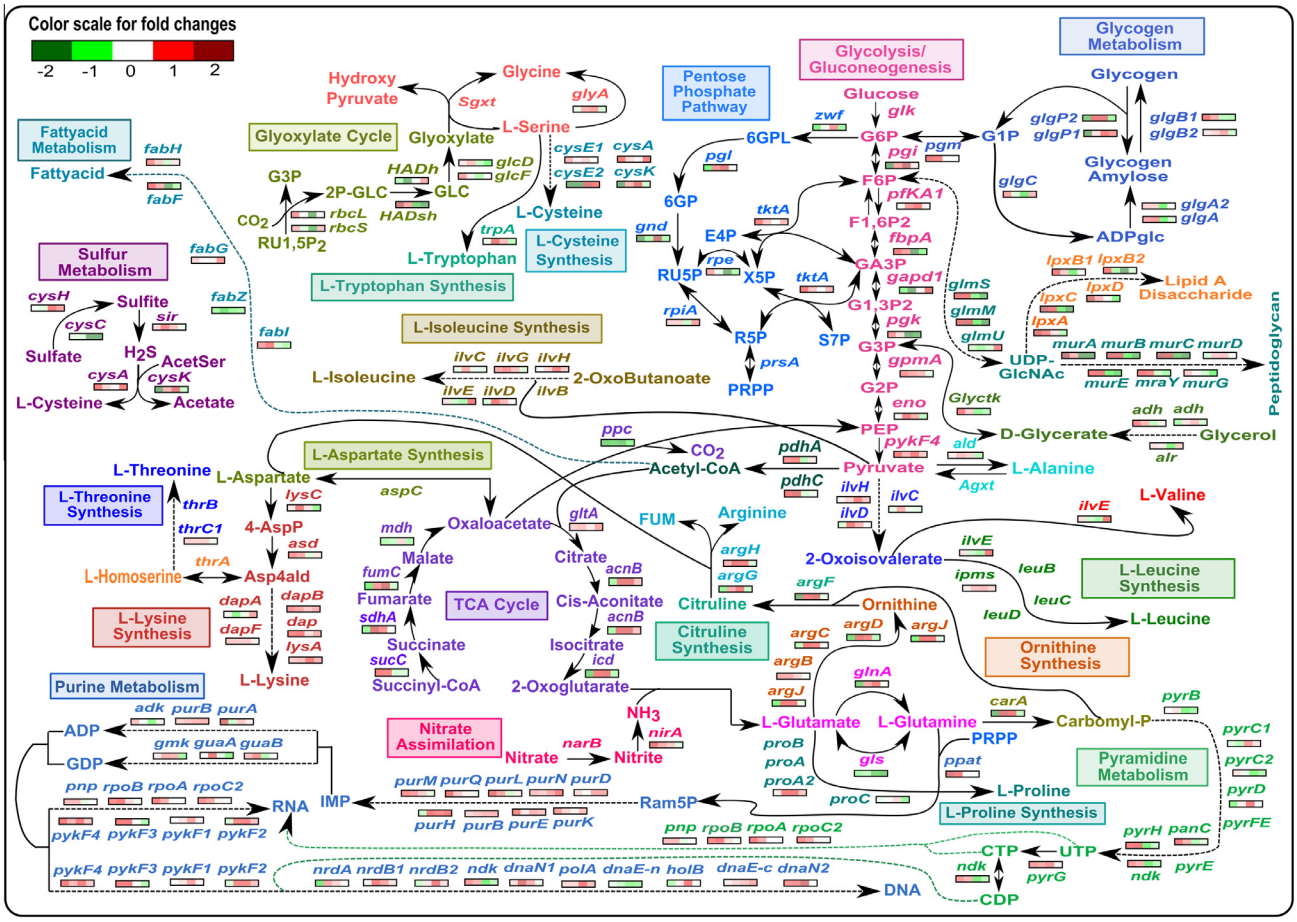

Fig. 4. Oscillation in central carbon pathways of *Cyanothece* 51142 under mixotrophy and nitrogen fixing conditions. Each filled bar in the pictorial layout depicts expression of an individual gene in color coded format at four time points; 1 h, 5 h, 13 h and 17 h in the 3rd day of diurnal cycle. The text immediately above each bar denotes the standard gene acronym for each of the individual genes. Scale bar on the top represents fold change values. Refer to legend to Fig. 2 for details. (For interpretation of the references to color in this figure legend, the reader is referred to the web version of this article.)

Interestingly, the final complex subunit ATP synthase in the ETC indicated a marked increase in the gene expression more than that in photoautotrophy (Stockel et al. 2008) mapped genes. This emphasized that the organism synthesizes more ATP molecules for efficiently driving the cellular metabolism in the presence of glycerol.

3.2.6. Glycogen metabolism

In glycogen metabolism, the genes that support glycogen synthesis, namely *glgA*, *glgA2*, *glgB1* and *glgB2* were observed strongly up-regulated at the day time (Fig. 4). This suggested that the combined effect of CO_2 uptake and glycerol consumption, would have contributed more carbon flux to synthesize large amount of glycogen granules as carbohydrate reserves. In fact, the glycogen content in mixotrophic condition showed higher concentration than that reported for photoautotrophic condition (Krishnakumar et al., 2013). Moreover, it seems that the metabolite G1P produced from G3P via gluconeogenesis served as a key substrate in synthesizing the glycogen granules. In agreement to this, the gene *pgm* (phosphoglucomutase) that catalyzes the conversion of G6P to G1P was identified as highly active during the day (Fig. 4). Alternatively, the glycogen degradation genes (*glgP1* and *glgP2*) started to up-regulate before the night fall so as to provide energy for nitrogen fixation. Similar to this, the biochemically measured glycogen content increased maximum during the day and decreased sharply well before the onset of darkness (Fig. 1). Also, the reductive pentose phosphate pathway that mediates glycogen degradation was identified active in converting G6P to GA3P. Further, the starting substrate G6P for pentose phosphate pathway was obtained through inter-conversion from G1P during glycogen catabolism. Intriguingly, the intracellular glycogen concentration remains lower and also does not oscillate under constant light (LL) at least till the time till the glycerol is present in the medium. This suggests that under the free running period, the culture might be majorly depending on glycerol, not only as a carbon source but also as a substrate to be oxidized so as to generate intracellular anoxic microenvironment for nitrogen fixation and hydrogen production.

3.2.7. Impact of glycerol on central carbon metabolism

Interestingly, addition of glycerol not only induced the central carbon metabolic pathways such as glycolysis, pentose phosphate pathway and TCA cycle, but also resulted in strong up-regulation of the genes in amino acid biosynthesis, purine and pyrimidine metabolism (Fig. 4) as compared to that under photoautotrophic growth (Stockel et al., 2008). In addition, the genes that are involved in fatty acid metabolism and peptidoglycan cell wall synthesis were also noticed to be upregulated, indicating a possible indirect effect of excess available carbon through glycogen breakdown being channelized to these pathways on account of glycerol feeding carbon into the central carbon metabolism mainly via glycolysis pathway. This suggests that the supplementation of glycerol effectively increases the carbon flux to the organism so as to involve in active

metabolism for faster cell growth and higher biomass production, with a potential to be tapped for channelizing to high value products including biofuels.

4. Conclusions

Supplementation of glycerol as an exogenous carbon source induced many vital cellular metabolic activities such as photosynthesis, nitrogen fixation, cell division, glycogen metabolism and central carbon metabolic pathways. Glycerol serves not only as an additional carbon source, but also seems to serve as a reducing substrate for providing the required anaerobic microenvironment for nitrogen fixation and hydrogen production. The results strongly suggest that with constitutive expression of the required proteins, constitutive hydrogen production should be achievable, with glycerol dispensing off the need for temporal compartmentalization of the otherwise mutually incompatible metabolic processes.

Acknowledgements

The work was partially funded by an Australia-India strategic research (AISRF) Grant to P.P.W. and M.C. The Grant to the Indian side was provided by Department of Biotechnology, Ministry of Science and Technology, Government of India, Grant number: BT/Indo-Aus/04/04/2009.

Appendix A. Supplementary data

Supplementary data associated with this article can be found, in the online version, at http://dx.doi.org/10.1016/j.biortech.2015.02.016.

References

Addinall, S.G., Lutkenhaus, J., 1996. FtsA is localized to the septum in an FtsZ-dependent manner. J. Bacteriol. 178 (24), 7167–7172.
Alagesan, S., Gaudana, S.B., Krishnakumar, S., Wangikar, P.P., 2013. Model based optimization of high cell density cultivation of nitrogen-fixing cyanobacteria. Bioresour. Technol. 148, 228–233.
Bandyopadhyay, A., Stockel, J., Min, H.T., Sherman, L.A., Pakrasi, H.B., 2010. High rates of photobiological H-2 production by a cyanobacterium under aerobic conditions. Nat. Commun. 1.
Bandyopadhyay, A., Elvitigala, T., Liberton, M., Pakrasi, H.B., 2013. Variations in the rhythms of respiration and nitrogen fixation in members of the unicellular diazotrophic cyanobacterial genus *Cyanothece*. Plant Physiol. 161 (3), 1334–1346.
Burnap, R.L., Nambudiri, R., Holland, S., 2013. Regulation of the carbon-concentrating mechanism in the cyanobacterium *Synechocystis* sp. PCC6803 in response to changing light intensity and inorganic carbon availability. Photosynth. Res. 118 (1–2), 115–124.
Carrieri, D., Wawrousek, K., Eckert, C., Yu, J., Maness, P.C., 2011. The role of the bidirectional hydrogenase in cyanobacteria. Bioresour. Technol. 102 (18), 8368–8377.
Cerveny, J., Nedbal, L., 2009. Metabolic rhythms of the cyanobacterium *Cyanothece* sp. ATCC 51142 correlate with modeled dynamics of circadian clock. J. Biol. Rhythms 24 (4), 295–303.
Cerveny, J., Sinetova, M.A., Valledor, L., Sherman, L.A., Nedbal, L., 2013. Ultradian metabolic rhythm in the diazotrophic cyanobacterium *Cyanothece* sp. ATCC 51142. Proc. Natl. Acad. Sci. USA 110 (32), 13210–13215.
Colon-Lopez, M.S., Sherman, D.M., Sherman, L.A., 1997. Transcriptional and translational regulation of nitrogenase in light-dark- and continuous-light-grown cultures of the unicellular cyanobacterium *Cyanothece* sp. strain ATCC 51142. J. Bacteriol. 179 (13), 4319–4327.
Cooley, J.W., Vermaas, W.F.J., 2001. Succinate dehydrogenase and other respiratory pathways in thylakoid membranes of Synechocystis sp. strain pcc 6803: capacity comparisons and physiological function. J. Bacteriol. 183 (14), 4251–4258.
Dean, D.R., Bolin, J.T., Zheng, L., 1993. Nitrogenase metalloclusters: structures, organization, and synthesis. J. Bacteriol. 175 (21), 6737–6744.
Elvitigala, T., Stockel, J., Ghosh, B.K., Pakrasi, H.B., 2009. Effect of continuous light on diurnal rhythms in *Cyanothece* sp. ATCC 51142. BMC Genomics 10, 226.
Feng, X., Bandyopadhyay, A., Berla, B., Page, L., Wu, B., Pakrasi, H.B., Tang, Y.J., 2010. Mixotrophic and photoheterotrophic metabolism in *Cyanothece* sp. ATCC 51142 under continuous light. Microbiology 156 (8), 2566–2574.
Gaudana, S.B., Krishnakumar, S., Alagesan, S., Digmurti, M.G., Viswanathan, G.A., Chetty, M., Wangikar, P.P., 2013. Rhythmic and sustained oscillations in metabolism and gene expression of *Cyanothece* sp. ATCC 51142 under constant light. Front. Microbiol. 4, 374.
Ghirardi, M.L., Posewitz, M.C., Maness, P.C., Dubini, A., Yu, J., Seibert, M., 2007. Hydrogenases and hydrogen photoproduction in oxygenic photosynthetic organisms. Annu. Rev. Plant Biol. 58, 71–91.
Gottesman, S., 2003. Proteolysis in bacterial regulatory circuits. Annu. Rev. Cell Dev. Biol. 19, 565–587.
Kinney, J.N., Axen, S.D., Kerfeld, C.A., 2011. Comparative analysis of carboxysome shell proteins. Photosynth. Res. 109 (1–3), 21–32.
Krishnakumar, S., Gaudana, S.B., Nguyen, X.V., Viswanathan, G.A., Chetty, M., Wangikar, P.P. Unpublished results. Coupling of cellular processes and their coordinated oscillations under continuous light in *Cyanothece* sp. ATCC 51142, a diazotrophic unicellular cyanobacterium.
Krishnakumar, S., Gaudana, S.B., Viswanathan, G.A., Pakrasi, H.B., Wangikar, P.P., 2013. Rhythm of nitrogen fixation by *Cyanothece* sp. ATCC 51142 under fully aerobic conditions. Biotechnol. Bioeng. 110, 2371–2379.
Leplat, C., Champeimont, R., Saenkham, P., Cassier-Chauvat, C., Jean-Christophe, A., Chauvat, F., 2013. Genome-wide transcriptome analysis of hydrogen production in the cyanobacterium *Synechocystis*: towards the identification of new players. Int. J. Hydrogen Energy 38 (4), 1866–1872.
McGinn, P.J., Jones, M.J., Macdonald, A.B., Campbell, D.A., 2005. Light is required for low-CO_2-mediated induction of transcripts encoding components of the CO_2-concentrating mechanism in the cyanobacterium *Synechococcus elongatus*: analysis by quantitative reverse transcription – polymerase chain reaction. Can. J. Bot. 83 (7), 711–720.
Min, H.T., Sherman, L.A., 2010. Hydrogen production by the unicellular, diazotrophic cyanobacterium *Cyanothece* sp strain ATCC 51142 under conditions of continuous light. Appl. Environ. Microbiol. 76 (13), 4293–4301.
Pils, D., Schmetterer, G., 2001. Characterization of three bioenergetically active respiratory terminal oxidases in the cyanobacterium *Synechocystis* sp. strain PCC 6803. FEMS Microbiol. Lett. 203 (2), 217–222.
Price, G.D., 2011. Inorganic carbon transporters of the cyanobacterial CO_2 concentrating mechanism. Photosynth. Res. 109 (1–3), 47–57.
Prince, R.C., Kheshgi, H.S., 2005. The photobiological production of hydrogen: potential efficiency and effectiveness as a renewable fuel. Crit. Rev. Microbiol. 31 (1), 19–31.
Reddy, K.J., Haskell, J.B., Sherman, D.M., Sherman, L.A., 1993. Unicellular, aerobic nitrogen-fixing cyanobacteria of the genus *Cyanothece*. J. Bacteriol. 175 (5), 1284–1292.
Schmetterer, G., Valladares, A., Pils, D., Steinbach, S., Pacher, M., Muro-Pastor, A.M., Flores, E., Herrero, A., 2001. The coxBAC operon encodes a cytochrome c oxidase required for heterotrophic growth in the cyanobacterium *Anabaena variabilis* strain ATCC 29413. J. Bacteriol. 183 (21), 6429–6434.
Schmitz, O., Kentemich, T., Zimmer, W., Hundeshagen, B., Bothe, H., 1993. Identification of the *nifJ* gene coding for pyruvate: ferredoxin oxidoreductase in dinitrogen-fixing cyanobacteria. Arch. Microbiol. 160 (1), 62–67.
Schneegurt, M.A., Sherman, D.M., Nayar, S., Sherman, L.A., 1994. Oscillating behavior of carbohydrate granule formation and dinitrogen fixation in the cyanobacterium *Cyanothece* sp. strain ATCC 51142. J. Bacteriol. 176 (6), 1586–1597.
Sherman, L., Min, H., Toepel, J., Pakrasi, H., 2010. Better living through cyanothece – unicellular diazotrophic cyanobacteria with highly versatile metabolic systems. In: Recent Adv. Phototrophic Prokaryotes, 675. Springer, New York, pp. 275–290.
Stockel, J., Welsh, E.A., Liberton, M., Kunnvakkam, R., Aurora, R., Pakrasi, H.B., 2008. Global transcriptomic analysis of Cyanothece 51142 reveals robust diurnal oscillation of central metabolic processes. Proc. Natl. Acad. Sci. USA 105 (16), 6156–6161.
Tamagnini, P., Leitao, E., Oliveira, P., Ferreira, D., Pinto, F., Harris, D.J., Heidorn, T., Lindblad, P., 2007. Cyanobacterial hydrogenases: diversity, regulation and applications. FEMS Microbiol. Rev. 31 (6), 692–720.
Toepel, J., Welsh, E., Summerfield, T.C., Pakrasi, H.B., Sherman, L.A., 2008. Differential transcriptional analysis of the cyanobacterium *Cyanothece* sp. strain ATCC 51142 during light-dark and continuous-light growth. J. Bacteriol. 190 (11), 3904–3913.
Vermaas, W.F.J., 2001. Photosynthesis and respiration in cyanobacteria. eLS, 1–7.